Growth and Erosion of Thin Solid Films

G. STEVEN BALES, ROBIJN BRUINSMA, ELLIOTT A. EKLUND, R. P. U. KARUNASIRI, JOSEPH RUDNICK, ANDREW ZANGWILL

Thin films that are grown by the process of sputtering are, by and large, quite unlike the smooth, featureless structures that one might expect. In general, these films have a complicated surface morphology and an extended network of grooves and voids in their interiors. Such features can have a profound effect on the physical properties of a thin film. The surface irregularities and the bulk defects are the result of a growth instability due to competitive shadowing, an effect that also plays a role in geological processes such as erosion. For amorphous thin films, the shadow instability can be described by a remarkably simple model, which can be shown to reproduce many important observed characteristics of thin film morphology.

MAN-MADE SOLID FILMS ARE UBIQUITOUS IN A TECHNOLOGICAL society. Everyday examples include "no-stick" coatings on frying pans, "no-glare" coatings on roadside signs, and "no-corrosion" coatings on garden tools. Less pedestrian, but not less important, examples include magnetic films for recording, conducting films for microelectronic contacts, and amorphous silicon films for photovoltaics. In the latter cases particularly, interest centers on films with thicknesses measured in the micrometer range, that is, "thin" on a macroscopic scale but still quite "thick" on a microscopic scale. Moreover, it is common to give up single crystallinity in exchange for thickness uniformity over macroscopic lateral dimensions. Perforce, these films exhibit an intrinsic microstructure that both depends on the details of fabrication and determines many of their physical properties (*1*).

A very common experimental technique used to produce films of this sort is known as sputtering (*2*). An energetic beam of particles (usually an inert gas) is directed at a bulk specimen of the material one wishes to deposit. The beam erodes this target, ejecting atoms that travel ballistically until they are deposited on a fixed substrate. The geometry can be arranged so that each point on the substrate receives flux either (in one extreme) from a fixed angle of incidence or (in another extreme) from all angles of incidence simultaneously. Moreover, one can easily imagine defocusing the original incident beam so that the particles incident on each point of the bulk target surface arrive from a range of angles as well. Surfaces that evolve under conditions of either sputter growth or sputter erosion exhibit characteristic morphologies that depend on the angular spread of the incident flux, the deposition rate, and the surface temperature.

G. S. Bales and A. Zangwill are in the School of Physics, Georgia Institute of Technology, Atlanta, GA 30332. R. Bruinsma, E. A. Eklund, R. P. U. Karunasiri, and J. Rudnick are in the Department of Physics, University of California, Los Angeles, CA 90024.

The purpose of this article is to review recent progress in our theoretical understanding of this behavior and, in particular, to emphasize certain statistical properties of moving interfaces that have a bearing on related problems in fields as diverse as geology, horticulture, and optics.

The ingredients essential to a proper theory of the morphological dynamics of sputter growth and erosion were understood qualitatively in the early 1950s. Konig and Helwig (*3*) pointed out in the optics literature that geometrical shadowing of an incident beam by protruding parts of a growing surface profoundly affects the resulting morphology, and Herring (*4*) emphasized in the metallurgical literature the importance of capillarity, or surface diffusion, as a driving force for morphological evolution. For the case of growth, precisely these factors have been invoked to explain the apparently "universal" classification scheme for thin-film microstructure illustrated in Fig. 1 (*5*). In particular, it is argued qualitatively (*6*) that shadowing leads to the zone 1 morphology of low-density tapered columns with domed tops, giving way (by surface diffusion) to wider, smoother uniform columnar grains (zone 2) and finally (by bulk diffusion) to large bulk-like grains (zone 3). Similarly, both shadowing and surface diffusion are important factors (*7*) in the evolution of rough "cone-like" surface topologies observed (*8*) during sputter erosion of contaminated surfaces. Repeated sputter-anneal cycles are, in fact, standard procedure for the preparation of "clean" surfaces for ultrahigh-vacuum studies (*9*).

Some years ago, computer simulations of "sticky" spheres constrained to approach a substrate on straight-line ballistic paths quantitatively established atomic scale self-shadowing as a mechanism for the formation of voided columnar microstructures (*10*). More recently, very large-scale simulations of this ballistic aggregation model revealed that the resulting deposits consist of quasi-fractal (*11*) tree-like structures riddled with holes on the atomic scale (*12*). Real coatings, by contrast, are smooth over distances less than approximately 10 nm, down to atomic scales—a range of two orders of magnitude. [The existence of surface variations on the atomic scale is, of course, a universal feature of all real surfaces (*10*).] This underscores the importance of smoothing by surface diffusion, an effect that can be included only rather crudely in atomistic simulations (*13*). Moreover, it is hardly practical to follow the motion of individual atoms if one is interested in macroscopic morphological evolution. One is thus led to consider continuum models that relinquish atomicity in favor of predictive power over large length and time scales.

A macroscopic description of growth and erosion, or both, often involves the construction of a partial differential equation to describe the time evolution of a surface profile $h(x,t)$ (Fig. 2). Carter (*14*) has reviewed a very elegant approach to this problem based on the construction of an eikonal equation (familiar from ray optics) for the motion of the (curved) surface and applied it most successfully to the case of sputter erosion. When the rate of erosion (or growth) of

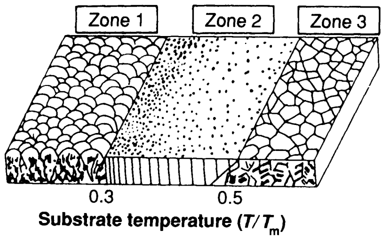

Fig. 1. Morphological classification of thin-film microstructure as a function of substrate temperature (scaled to the melting point) (*5*).

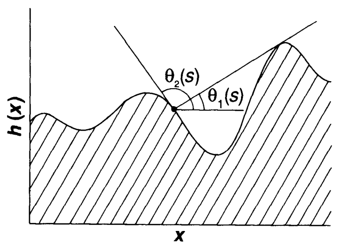

Fig. 2. Typical surface profile $h(x)$. Incident particles can reach the point x ballistically from all directions within the cone defined by the angles $\theta_1(s)$ and $\theta_2(s)$ (s is the arc length along the surface).

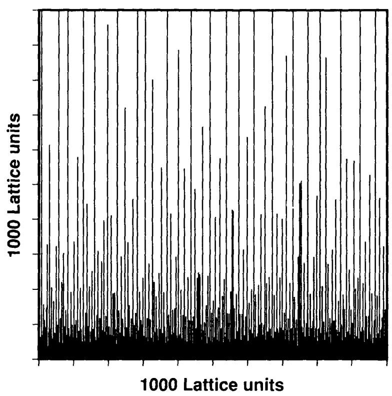

Fig. 3. Growth pattern for the grass model.

a surface point is assumed to be constant, the method of characteristics can be used to predict the appearance of singularities (such as caustics) in the evolving surface. Kardar and co-workers (*15*) have advanced a version of this model specifically for the case of vapor deposition. However, by construction, this local theory contains no shadowing and so cannot lead to columnar microstructures. Until recently, columnar structures have been derived from continuum models only when microscopic information is built in at the monolayer level (*16, 17*).

Growth with Shadowing

A crude model for the growth of a grassy lawn nicely illustrates the dramatic effects of shadowing. Let us represent every blade of grass as a column on a lattice. Now suppose that each stalk grows at a rate proportional to the amount of light it receives at its tip. On a cloudless day, this amount will be proportional to the solid angle of sky that is not blocked by neighboring stalks. This growth rule is easy to study on a computer (*18*). Figure 3 shows the result for initial "seedlings" that differ in height by infinitesimally small amounts (for the case of a one-dimensional strip of grass). The shortest stalks quickly "lose" as they are overshadowed and choked off by their taller neighbors. The "winners" compete among themselves for the available light until a limiting morphology is achieved that exhibits elements of both regularity and randomness. (Unattended lawns are indeed known to acquire an uneven appearance.)

In this simple model, the regularity derives from the nature of the height distribution of columns. Let a be the unit of column height. Then, if there are N columns of height a, one finds that there are $N/2$ columns of height $2a$, $N/4$ columns of height $4a$, and so forth. The final morphology turns out to be "self-similar" and to exhibit "scaling" characteristics. This means that any small portion of Fig. 3 that is rescaled (magnified) to full size is indistinguishable from the original pattern. Remarkably, actual sputter-grown solid films also appear to be self-similar (*19*), or, more precisely, they are self-similar down to some minimum size where, as noted earlier, surface diffusion takes over.

To adequately account for this behavior, we require a growth algorithm that captures the effects of both shadowing and surface diffusion. A fairly realistic way to do this (taking no account of any atomistic effects) is the following (*20*). Each point on the surface is presumed to grow in the direction of the local surface normal $\hat{n}(s)$ at a rate

$$v_n(s) = R \int_{\theta_1(s)}^{\theta_2(s)} \mathbf{J}(\alpha) \cdot \hat{n}(s)\, d\alpha + D \frac{\partial^2 \kappa(s)}{\partial s^2} \tag{1}$$

In this expression, the shadow angles $\theta_1(s)$ and $\theta_2(s)$ are defined in Fig. 2; R is the mean deposition rate, equal to the molecular flux, multiplied by the atomic volume of the species being deposited; and $\mathbf{J}(\alpha)$ is a dimensionless vector that characterizes the angular dependence of the incident flux. Surface diffusion contributes to the growth rate by an amount equal to the divergence of the surface diffusion current, $-D[\partial\kappa(s)/\partial s]$, where $\kappa(s)$ is the surface curvature and s is the arc length along the surface. The constant D is proportional to the surface diffusion constant (*21*). In the absence of diffusion, Eq. 1 has been extensively used in computer simulations of sputter deposition onto patterned substrates for microelectronics applications (*22*).

Figure 4 illustrates the morphological evolution of a surface initially composed of three "nucleation sites," obtained by numerical evaluation of Eq. 1 for the case of uniform exposure (as for the grassy lawn) (*23*). The figure best represents the growth of an amorphous material, because we have neglected all effects of crystallinity. At early times, before shadowing becomes important, each protrusion grows upward and outward in a manner reminiscent of a classical wave front. This is consistent with the eikonal equation analysis (*14*). Later, all the characteristic features of a zone 1 microstructure appear: tapered columns with domed tops interlaced with a fine void network.

The natural selection process demonstrated by the simple grass model is evident: initial protrusions that are slightly larger than their neighbors tend to "win." Does growth according to Eq. 1 exhibit self-similar behavior, like the grass model? It is not known for certain because the computations required to test the long-time statistical properties simply take too much time. If, however, we approximate Eq. 1 by the eikonal equation (or Huygens principle) (*14*), then self-similar morphologies are found (*24*).

The initial conditions clearly play a fundamental role in Fig. 4 (*23, 24*). As mentioned, the shadow mechanism magnifies initial surface roughness. As a demonstration of the mathematical importance of the initial conditions (*23*), note that Eq. 1 contains a basic length scale ℓ_0 and a basic time scale t_0 defined by

$$\ell_0 = (D/R)^{1/3} \tag{2}$$

$$t_0 = \ell_0/R \tag{3}$$

We now can define a dimensionless length ℓ/ℓ_0 and a dimensionless time t/t_0. Rewriting Eq. 1 in these dimensionless variables leads to a parameter-free evolution equation (namely, Eq. 1 with $D = R = 1$). Accordingly, the only way to obtain fundamentally different growth

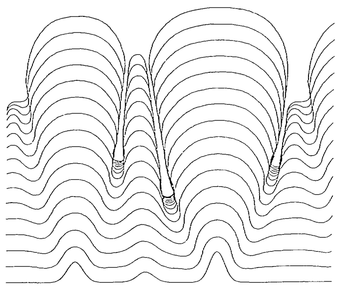

Fig. 4. Growth of a surface according to Eq. 1 [from (*23*)].

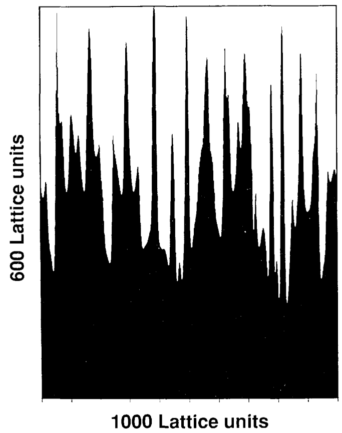

Fig. 5. Growth pattern for the grass model including surface diffusion (Eq. 4).

morphologies, that is, not related by a trivial change of scale, is to vary the morphology of the initial surface. The initial conditions were also found to be crucially important for growth controlled by the Huygens principle (*24*).

The foregoing immediately implies that we require a quantitative way to characterize the initial conditions. We will not do this directly for Eq. 1. Instead, we construct a simpler equation of motion that is, both mathematically and numerically, more tractable. In particular, we generalize the strictly columnar grass model to include the effects of surface diffusion (not present in real grass). The resulting equation of motion for the coating profile is (*18*):

$$\frac{\partial h}{\partial t} = |\theta_2(x) - \theta_1(x)| - \frac{\partial^2 \kappa}{\partial s^2} \tag{4}$$

where we have already passed to dimensionless variables. Equation 4 differs from Eq. 1 in a number of respects (*20*) but still captures the competition between shadowing and diffusion. Moreover, its numerical simulation is far less computer-intensive.

To characterize the initial state of the surface, we introduce two length scales. First, let ζ_0 be the lateral correlation length of the initial surface; that is, the initial surface is smooth on length scales less than ζ_0 and rough on length scales greater than ζ_0. For instance, ζ_0 could be the size of microcrystallites in the amorphous film. Next, let Δh be the root mean square (rms) of the height fluctuations of the initial surface. Together, Δh and ζ_0 provide an (approximate) characterization of the statistical properties of the initial surface. It follows from Eq. 4 that, for the initial surface, the second term can be estimated as $\ell_0^3\ (\Delta h/\zeta_0^4)$. Now let $\Delta\theta \equiv [\langle\theta^2\rangle - \langle\theta\rangle^2]^{1/2}$ be the rms of the fluctuations in the exposure angle. Because θ varies between π and $\pi - 2\tan^{-1}(\Delta h/\zeta_0)$, we can estimate $\Delta\theta \approx \tan^{-1} \Delta h/\zeta_0$. The (time-dependent) ratio $\mathcal{P}$ of the surface diffusion term in Eq. 1 to the rms fluctuations in the deposition current then is roughly

$$\mathcal{P} = \left(\frac{\ell_0}{\zeta_0}\right)^3 \left[\frac{\Delta h/\zeta_0}{\tan^{-1}(\Delta h/\zeta_0)}\right] \tag{5}$$

If $\mathcal{P}$ is large compared to unity, we expect surface diffusion to largely erase the initial structure, whereas, if $\mathcal{P}$ is small compared to unity, we expect magnification through shadowing of the initial surface roughness.

Figure 5 illustrates the growth profile for a case in which the initial $\mathcal{P}$ value, $\mathcal{P}_0$, was equal to 1, that is, there is nonnegligible surface diffusion. The initial surface was taken as a collection of columns of width ζ_0 and rms height Δh. Characteristically, the surface remains quite flat for some induction period before columns begin to appear. Compared to the pattern in Fig. 3, there are fewer and wider columns. A convenient measure of the statistical properties of such a surface is the coverage $c(h)$, defined simply as the fraction of area (or length in the one-dimensional examples discussed here) occupied by coating in a layer parallel to the substrate at a height between h and $h + dh$. For a smooth, high-quality film of uniform thickness, $c(h)$ drops abruptly from unity to zero when $h = h_m$. Conversely, $c(h)$ is expected to fall smoothly to zero for a low-quality (rough) surface. As a benchmark, we note that $c(h) \propto 1/h$ for the maximally rough self-similar surface of Fig. 3.

Numerical studies indicate (*18*) that, if the control parameter $\mathcal{P}_0$ is small compared to unity, the film evolves smoothly up to an induction height h^*. For $h \gtrsim h^*$, the film roughens and $c(h) \propto 1/h^p$ for $h > h^*$. The exponent p has a value between 1 and 2 depending on $\mathcal{P}_0$. For very large h, there is a cutoff for this power-law regime. As for the original grass model, the surface profile is self-similar.

If, on the other hand, $\mathcal{P}_0$ is large compared to unity, then, as long as the film could be followed by us on the computer, $c(h) \approx 1$ up to a film height $h^* \propto t$. For $h > h^*$, $c(h)$ dropped rapidly. The width of the surface did, however, slowly increase in time, so we cannot rule out that for very late times a self-similar mountain surface would appear. With this caveat in mind, it indeed appears that $\mathcal{P}_0$ is suitable as a characterization for the initial surface. Finally, if we study the time dependence of $\mathcal{P}(t)$, we find that $\mathcal{P}(t)$ decreases with time if $\mathcal{P}_0 > 1$, whereas it increases with time if $\mathcal{P}_0 < 1$. For late times, $\mathcal{P}(t)$ always is of order one. This indicates that (at least for the growth according to Eq. 4) ultimately the surface always achieves a balance between surface diffusion and shadowing.

The fact that the surface morphology is very sensitive to initial conditions is somewhat reminiscent of nonlinear classical mechanics problems that exhibit chaos (*25*). We also can think of the discretized version of Eq. 4 as a nonlocal cellular automaton. Indeed, cellular automata are known to be sensitive to the initial state and to evolve self-similar or homogeneous growth patterns (*26*).

The transition from a smooth surface (for $\mathcal{P}_0 \gtrsim 1$) to a rough surface (for $\mathcal{P}_0 \lesssim 1$) corresponds to a "growth-induced" roughening transition (as opposed to a temperature-induced roughening transition), a subject of great interest in the recent literature (*27*). However, even for our simplified model (Eq. 4), we cannot follow the surface to late times because of numerical limitations. In particular, it is difficult to distinguish numerically a slow coarsening process that is sensitive to initial conditions from a true growth-induced roughening transition.

Erosion

The action of wind and rain on a mountain range is the analog to the grassy lawn for the problem of the evolution of a solid surface under energetic ion bombardment. Erosion corresponds to negative values for the parameter R in Eq. 1, while landslides play the role of surface diffusion. In contrast to growth, shadowing always leads to surface smoothing during erosion. It is particularly effective when the topography is very rough, because deep valleys are well shielded from the elements. Typically, erosion acts as a smoothing mechanism (even in the absence of shadowing), because, according to Eq. 1, each bit of hilly area erodes along the direction of the local surface normal (Huygens principle) (*28*). Explicit calculations of soil erosion exploiting this fact have appeared in the geomorphology literature (*29*), but the role of shadowing is less well understood.

For the case of true sputter erosion (in the absence of surface diffusion), extensive numerical simulations based on a generalized Huygens principle of wave propagation have been performed with particular emphasis on the evolution of sharp corners and edges in the initial surface profile (*30*). Using Eq. 1, Kubby and Siegel (*31*) studied the effects of surface diffusion on the erosion of macroscopic features and obtained results that compare favorably with experimental results. In what follows, we shall emphasize the microscopic statistical aspects of the problem. To begin, Fig. 6A illustrates typical erosion dynamics obtained by numerical integration of Eq. 4 for the case of uniform exposure to an (isotropic) incident flux. A rather hilly starting surface has been chosen so that both shadowing and capillarity are significant. Surface diffusion provides smoothing over short length scales, and shadowing induces preferential erosion of all local maxima.

We now introduce the fact that the incident flux unavoidably exhibits statistical fluctuations around its average value (R) due to the fact that the beam actually consists of discrete atoms. This phenomenon, known as "shot noise," can be modeled adequately simply by the addition of a Gaussian random variable $\eta(x,t)$ to the right side of Eq. 4. The effect of this change can be quite profound. Take the case of an initially flat surface where (in the absence of noise) one obtains perfectly uniform erosion. In the presence of shot noise, something entirely different occurs (Fig. 6B): large-scale mountain-like structures evolve at long times. Qualitatively, it is clear that any energetic incident beam continually produces surface damage, mostly on the atomic scale. Occasionally, larger structures are produced as a result of shot noise fluctuations. Sputter bombardment slowly erodes these structures, but other, new ones are constantly being produced. Eventually, a steady state is reached, precisely as observed (*32*) in detailed experiments addressed to the evolution of the "cone-like" structures during erosion noted earlier.

More quantitatively, one can do a Fourier analysis of the eroding surface profile $h(x,t)$ and study instead the time evolution of each component $h_q(t)$ characterized by a wave vector q. When the slopes of the mountain structures are not too large, the results of such an analysis can be calculated from linear response theory applied to Eq. 4 with $R < 0$.

$$\langle |h_q(t)|^2 \rangle \propto \frac{\langle |\eta_q|^2 \rangle}{Dq^4 + \alpha R|q|}(1 - e^{-2(Dq^4 + \alpha R|q|)t}) \qquad (6)$$

where α is a numerical constant and the Fourier transform of the

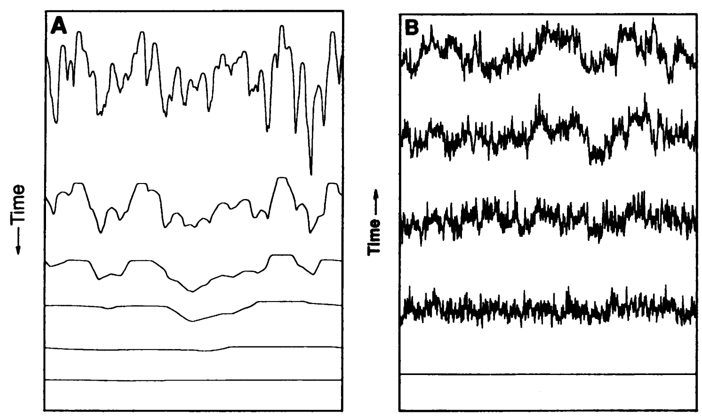

Fig. 6. (**A**) Erosion of an initially rough surface according to Eq. 4; (**B**) erosion of an initially flat surface including shot noise in the incident flow.

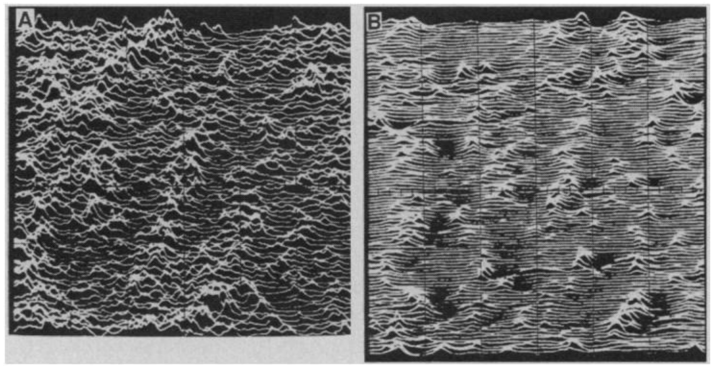

Fig. 7. (**A**) Scanning tunneling microscope image of a flat carbon surface after exposure to 5-keV ions for 15 min at a beam current of $R = 6.4$ μA; (**B**) same as (A) but after exposure for 150 min at $R = 0.64$ μA.

standard deviation of the random variable $\langle |\eta_q|^2 \rangle \propto R$.

Equation 6 tells us two things. First, for $t \rightarrow \infty$, it directly implies steady-state roughness of large (lateral) scale. To see this, start with a surface characterized by small-amplitude, noise-induced roughness of all wavelengths. For large t, the long-wavelength Fourier components increase in amplitude as a result of divergence of $\langle |h_q(\infty)|^2 \rangle$ when $q \rightarrow 0$. (This divergence is in reality limited by finite-size effects and nonlinear corrections to linear response theory.)

Equation 6 also makes clear that the height fluctuations depend on R only in the combinations D/R and Rt. This fact (another consequence of the rescaling properties of our model) means that variations in surface diffusion can be simulated by reciprocal changes in R and t so that the product Rt remains fixed. We have tested this prediction for the sputter erosion case by means of scanning tunneling microscopy (STM) (*33*). Figure 7A is an image of an initially flat carbon surface roughened by exposure to 5-keV Ar^+ ions for $t = 15$ min at a beam current of $R = 6.4$ μA. Figure 7B displays the image obtained for a flat carbon surface bombarded for $t = 150$ min with $R = 0.64$ μA.

In accordance with Eq. 6, the erosion process has produced large-scale structures. Furthermore, the change in erosion rate between Figs. 7A and 7B should be equivalent to keeping R and t fixed while increasing D by a factor of 10 according to Eq. 6. This in turn means that the short-scale structure should be erased in going from Fig. 7A to Fig. 7B while the large-scale structure should be unaffected. Inspection of Fig. 7 shows that this is the case, at least qualitatively.

Another useful measure of interface roughness is the interfacial width $W(L)$ defined for a sample of lateral dimension L (*34*). For columnar models, $W(L)$ is simply a mean square average:

$$W^2(L) = \frac{1}{N}\sum_{i=1}^{N} [h(x_i) - \langle h \rangle]^2 \qquad (7)$$

where N is the total number of columns. The long-time behavior of this quantity for an eroding surface follows from Eq. 4 as

$$W^2(L) \propto \sum_{q > 1/L} \langle |h_q(\infty)|^2 \rangle \propto \ell n(L/\ell_0) \qquad (8)$$

Noise-induced roughness thus diverges as $L \rightarrow \infty$. But, because the logarithm increases so slowly, typical laboratory samples actually will appear reasonably smooth. It is interesting to contrast this behavior with the behavior of the interface width for the case of growth. There, one finds that $W(L) \propto L^{\chi}$ where

$$\chi = (2 - p)/2 \qquad (9)$$

and p is the growth exponent or $c(h)$ defined earlier. The rapid power-law divergence of $W(L)$ directly reflects the appearance of columnar microstructures due to shadowing. It also explains why we did not introduce shot noise in the context of growth. These fluctuations introduce only a negligible perturbation to the roughness induced by shadowing.

Concluding Remarks

In this article, we have discussed a macroscopic theoretical approach to the morphological evolution of thin films grown or eroded by sputtering. Particular emphasis has been placed on the effects of shadowing, shot noise, and the statistical properties of these films. To motivate our discussion, we noted the similarity of our problem both to the growth of grass and to the erosion of mountains. To see the connection to still other problems, it is useful to examine results obtained in the statistical mechanics literature for growth onto a flat substrate according to the so-called Eden (*35*) and diffusion-limited aggregation (DLA) (*12*) algorithms. In the first of these, new particles are attached sequentially to randomly chosen surface sites of the growing film. A compact but rough interface results. In the second, new particles released from above perform a random walk and join the film at their first point of contact. The growth surface is very ramified and is, in fact, fractal.

As defined, both of these models include shot noise but neither has a relaxation (smoothing) mechanism. Conversely, we have argued that the morphologies obtained by sputter deposition depend strongly on surface diffusion but only weakly on noise. To facilitate comparison, we take advantage of the fact that the behaviors of both DLA and the Eden model are known if noise is suppressed and relaxation is introduced. (The continuum limit of the noise-free Eden model is just the Huygens principle). For the Eden case, thought to be relevant to a common operating limit of the chemical vapor deposition process (*36*), all initial surfaces ultimately evolve into a collection of parabolic shock fronts, whose curvature decreases uniformly as time proceeds (*24*). The asymptotic surface is flat. Conversely, DLA modified in this manner yields (*37*) nonfractal finger-like morphologies. An example is provided by "viscous fingering," when air displaces a fluid trapped between two closely spaced glass panes (*38*). As the interface moves, larger fingers suppress smaller fingers until, asymptotically, only one finger remains.

Examination of Figs. 4 and 5 reveals that shadow growth exhibits characteristics of both the Eden and DLA models in the appropriate limits. At early times, before shadowing becomes important, surface features grow upward and outward like an Eden interface. But, as competition for incident flux ensues, there is a crossover to the finger-like morphology of the fluid problem and asymptotic survival by just a few columns. Evidently, there is a deep connection between the nonlocal shadowing that obtains for ballistic incident flux and the nonlocal screening that occurs for diffusive particle transport.

A quantitative comparison between the theory discussed here and experiment remains to be done. In particular, it is not known whether $\mathcal{P}$ is indeed the control parameter for the quality of a film. Nonetheless, as mentioned earlier, there is experimental evidence (*19*) that scaling persists for ballistic deposition, at least in some situations.

We believe that the type of analysis discussed here for the growth and erosion of thin films may be useful in other contexts as well. For example, it is tempting to speculate whether the interfacial width $W(L)$ of the canopy of a tropical rain forest (on the assumption that growth is limited by competition for sunlight) would exhibit power-law behavior. A statistical approach to the properties of eroding surfaces may also be interesting in the context of sandblasting, chemical etching and (perhaps) acid rain. Indeed, one can adopt a morphological perspective for each of the many examples in nature where growth or death occurs by a simple nutrient or poison transport mechanism. From this point of view, the rather modest case of sputtering treated here is merely representative.

REFERENCES AND NOTES

1. I. J. Hodgkinson and P. W. Wilson, *CRC Crit. Rev. Solid State Mater. Sci.* **15**, 27 (1988).
2. J. L. Vossen and W. Kern, Eds., *Thin Film Processes* (Academic Press, New York, 1978).
3. H. Konig and G. Helwig, *Optik* **6**, 111 (1950).
4. C. Herring, in *The Physics of Powder Metallurgy*, W. E. Kingston, Ed. (McGraw-Hill, New York, 1951), pp. 143–179.
5. B. A. Movchan and A. V. Demchishin, *Phys. Met. Metallogr. USSR* **28**, 83 (1969).
6. J. A. Thornton, *Annu. Rev. Mater. Sci.* **7**, 239 (1977).
7. S. M. Rossnagel, in *Erosion and Growth of Solids Stimulated by Atom and Ion Beams*, G. Kiriakidis, G. Carter, J. L. Whitton, Eds. (Nijhoff, Dordrecht, 1986), pp. 181–199.
8. R. S. Williams, R. J. Nelson, A. R. Schlier, *Appl. Phys. Lett.* **36**, 827 (1980).
9. A. Zangwill, *Physics at Surfaces* (Cambridge Univ. Press, Cambridge, 1988), pp. 27–28.
10. H. J. Leamy and G. H. Gilmer, in *Current Topics in Materials Science*, E. Kaldis, Ed. (North-Holland, Amsterdam, 1980), vol. 6, pp. 309–344.
11. B. B. Mandelbrot, *The Fractal Geometry of Nature* (Freeman, New York, 1983).
12. P. Meakin, *CRC Crit. Rev. Solid State Mater. Sci.* **13**, 143 (1987).
13. K. H. Muller, *J. Appl. Phys.* **58**, 2573 (1985).
14. G. Carter, in *Erosion and Growth of Solids Stimulated by Atom and Ion Beams*, G. Kiriakidis, G. Carter, J. L. Whitton, Eds. (Nijhoff, Dordrecht, 1986), pp. 70–97.
15. M. Kardar, G. Parisi, Y.-C. Zhang, *Phys. Rev. Lett.* **56**, 889 (1986).
16. S. Lichter and J. Chen, *ibid.*, p. 1396.
17. A. Mazor, D. J. Srolovitz, P. S. Hagan, B. G. Bukiet, *ibid.* **60**, 424 (1988).
18. R. P. U. Karunasiri, R. Bruinsma, J. Rudnick, *ibid.* **62**, 788 (1989).
19. R. Messier and J. E. Yehoda, *J. Appl. Phys.* **58**, 3739 (1985).
20. G. S. Bales and A. Zangwill, *Phys. Rev. Lett.* **63**, 692 (1989).
21. W. W. Mullins, *J. Appl. Phys.* **28**, 333 (1957). The constant $D = D_s\Omega^2r\gamma/k_BT$, where D_s is the surface diffusion constant, Ω is the atomic volume, r is the area density of surface atoms, γ is the surface tension, k_B is the Bolzmann constant, and T is the absolute temperature.
22. H. P. Bader and M. A. Lardon, *J. Vac. Sci. Technol. B* **4**, 833 (1986).
23. G. S. Bales and A. Zangwill, in preparation.
24. C. Tang, S. Alexander, R. Bruinsma, *Phys. Rev. Lett.* **64**, 772 (1990).
25. P. Berge, Y. Pomeau, C. Vidal, *Order Within Chaos* (Wiley, New York, 1984).
26. S. Wolfram, *Rev. Mod. Phys.* **55** (no. 3), 601 (1983).
27. Conference Proceedings of the NATO Advanced Research Workshop on *Kinetics of Ordering and Growth at Surfaces*, Aquafredda di Maratea, 1989 (Plenum, New York, in press).
28. The same effect, applied in the opposite direction for growth, is responsible for the expanding wave-front behavior evident in Fig. 4. For a discussion, see, for example, (*14*).
29. G. Carter and M. J. Nobes, *Earth Surface Processes* **5**, 131 (1980).
30. I. V. Katardjiev, *J. Vac. Sci. Technol. A* **6**, 2434 (1988).
31. J. A. Kubby and B. M. Siegel, in *Erosion and Growth of Solids Stimulated by Atom and Ion Beams*, G. Kiriakidis, G. Carter, J. L. Whitton, Eds. (Nijhoff, Dordrecht, 1986), pp. 444–452.
32. J. L. Whitton, *ibid.*, pp. 151–173.
33. E. A. Eklund, R. S. Williams, E. J. Snyder, in preparation.
34. F. Family and T. Vicsek, *J. Phys. A Math. Gen.* **18**, L75 (1985).
35. M. Eden, in *Proceedings of the Fourth Berkeley Symposium on Mathematics, Statistics, and Probability*, F. Neyman, Ed. (Univ. of California Press, Berkeley, 1961), vol. 4.
36. G. S. Bales, A. C. Redfield, A. Zangwill, *Phys. Rev. Lett.* **62**, 776 (1989).
37. S. Liang, *Phys. Rev. A* **33**, 2663 (1986).
38. J. H. S. Hele-Shaw, *Nature* **58**, 34 (1898).

39. We thank R. S. Williams for many fruitful discussions and, in particular, for bringing the STM experiments to our attention. The experimental work was supported by the Office of Naval Research.